J Therm Anal Calorim (2011) 103:365–372
DOI 10.1007/s10973-010-0777-x

Heat capacities and thermodynamic properties of MgNDC

Li-Fang Song · Cheng-Li Jiao · Chun-Hong Jiang · Jian Zhang · Li-Xian Sun · Fen Xu · Qing-Zhu Jiao · Yong-Heng Xing · F. L. Huang · Yong Du · Zhong Cao · Fen Li · Jijun Zhao

Received: 24 February 2010 / Accepted: 29 March 2010 / Published online: 6 May 2010

Abstract One-three-dimensional metal-organic frameworks $Mg_{1.5}(C_{12}H_6O_4)_{1.5}(C_3H_7NO)_2$ (MgNDC) has been synthesized solvothermally and characterized by single crystal XRD, powder XRD, FT-IR spectra. The low-temperature molar heat capacities of MgNDC were measured by temperature modulated differential scanning calorimetry (TMDSC) over the temperature range from 205 to 470 K for the first time. No phase transition or thermal anomaly was observed in the experimental temperature range. The thermodynamic parameters of MgNDC such as entropy and enthalpy relative to reference temperature of 298.15 K were derived based on the above molar heat capacities data. Moreover, the thermal stability and decomposition of MgNDC was further investigated through thermogravimetry (TG)–mass spectrometer (MS). Three stages of mass loss were observed in the TG curve. TG–MS curve indicated that the oxidative degradation products of MgNDC are mainly H_2O, CO_2, NO, and NO_2.

Keywords Magnesium · TMDSC · Metal-organic frameworks · Molar heat capacity · TG

L.-F. Song · C.-L. Jiao · C.-H. Jiang · J. Zhang · L.-X. Sun (✉)
Materials and Thermochemistry Laboratory, Dalian Institute of Chemical Physics, Chinese Academy of Sciences, 457 Zhongshan Road, Dalian 116023, People's Republic of China
e-mail: lxsun@dicp.ac.cn

L.-F. Song · C.-L. Jiao · C.-H. Jiang · F. Li
Graduate School of the Chinese Academy of Sciences, Beijing 100049, People's Republic of China

F. Xu (✉) · Q.-Z. Jiao · Y.-H. Xing
Faculty of Chemistry and Chemical Engineering, Liaoning Normal University, Dalian 116029, People's Republic of China
e-mail: xufen@lnnu.edu.cn

F. L. Huang
State Key Laboratory of Explosion Science and Technology, Beijing Institute of Technology, Beijing 100081, People's Republic of China

Y. Du
State Key Laboratory of Powder Metallurgy, Central South University, Changsha 410083, People's Republic of China

Z. Cao
College of Chemistry and Biological Engineering, Changsha University of Science and Technology, Changsha 410076, People's Republic of China

J. Zhao
Laboratory of Materials Modification by Laser, Electron, and Ion Beams, Dalian University of Technology, Dalian 116024, China

Introduction

Metal-organic frameworks (MOFs) have attracted a great deal of interests recently. Well-designed MOFs can bear interesting topologies and their specific structures have potential applications in gas storage [1], catalysis [2], chemical sensor [3], separation [4], medicine assay [5], and biological analysis [6]. This series of materials are generally constructed by transitional metal ions and polyfunctional organic linkers. However, alkali metals [7, 8] or alkaline-earth metals [9] constructed MOFs are rarely investigated. Actually, these light metals have the priority in building frameworks with light volumetric density and novel topology.

Heat capacities determinations of various compounds have attracted many researchers' attention [10–12]. Molar heat capacities of the materials at different temperatures

are basic data in chemistry and engineering, from which many other thermodynamic properties such as enthalpy and entropy can be calculated. Modulated differential scanning calorimetry (MDSC) is one of the easier and more accurate method for determining the heat capacity. The structure and principle of the calorimeter have been described in detail by the literatures [13–15]. This method has been greatly developed for directly determining heat capacities for various materials [16, 17] nowadays.

In this paper, we report one alkaline-earth MOFs named MgNDC, the low-temperature molar heat capacity of which was measured by TMDSC and the thermodynamic parameters such as entropy and enthalpy were also calculated. The accuracy of TMDSC was established by comparing the measured heat capacities of standard sapphire (α-Al_2O_3) with previously reported values (NIST and NBS) [18, 19]. The thermal decomposition characteristics of the compound were investigated by TG–MS.

Experimental

Sample

All chemicals and reagents were commercially available of analytical grade and were used as received. MgNDC has been synthesized by solvothermally reaction. 0.5 mmol 2,6-naphthalene dicarboxylic acid (0.22 g) and 1.0 mmol Mg $(NO_3)_2{\cdot}6H_2O$ (0.26 g) were dissolved in 20 mL *N*,*N*-dimethyllformamide (DMF), then 5 mL chlorobenzene was added to the solution under a vigorous stirring. The mixture was transferred into a 40 mL Teflon-lined stainless steel autoclave and heated at 383 K for 24 h, then cooled to room temperature naturally. After filtration, the product was washed with DMF thoroughly and then dried at 323 K in vacuum overnight. Straw yellow block crystals suitable for single crystal X-ray diffraction analysis were obtained in ca. 60% yield based on Mg(II).

Characterization

The crystal data were collected at 293 K using a SMART APEX II-CCD single crystal XRD (graphite monochromated Mo Kα radiation, $\lambda = 0.71073$ Å). A multi-scan absorption correction was applied using the SADABS program. The structures were solved by direct method and refined by full-matrix least-squares method implemented in SHELXTL-97 [20]. All the non-hydrogen atoms were refined anisotropically. Hydrogen atoms were added theoretically. Crystal data for the complex are as follows: $C_{24}H_{23}N_2O_8Mg_{1.5}$, $M_r = 503.92$, monoclinic system, *C*2/*c* (no. 15), $a = 13.4045(16)$ Å, $b = 18.0595(19)$ Å, $c = 20.928(2)$ Å, $\beta = 99.895(6)°$.

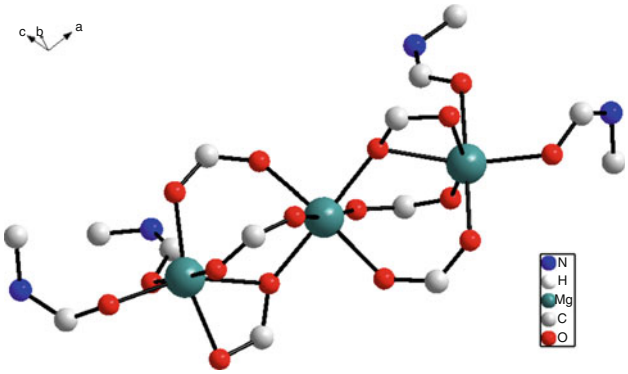

Fig. 1 Coordination environment of Mg atom

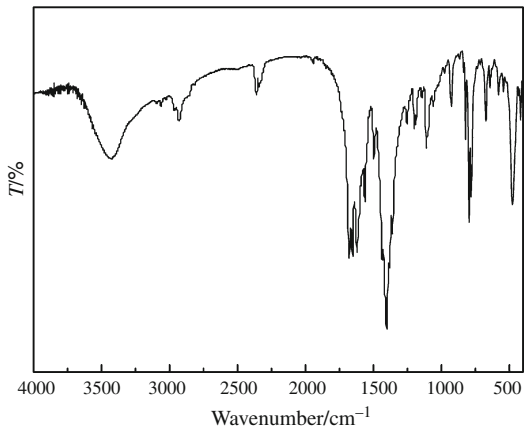

Fig. 2 IR spectrum of MgNDC

The asymmetric unit and metal coordination of MgNDC is shown in Fig. 1.

FT-IR spectra were recorded on a Nicolet 380 FT-IR spectrometer using KBr pellet in the wavenumber range of 4000–400 cm^{-1}. *v*: 3431 (m), 2929 (w), 1678 (s), 1655 (s), 1619 (s), 1561 (m), 1498 (m), 1434 (s), 1403 (s), 1359 (m), 1253 (w), 1200 (w), 1111 (w), 823 (w), 796 (s), 782 (s), 672 (w), 477 (s), 419 (w). The spectrum is shown in Fig. 2.

The purity of MgNDC was determined by the powder XRD. The program Mercury 1.4.2 was used for calculation of X-ray crystallographic powder patterns of MgNDC. Powder XRD experiments were carried out on a PANalytical X-ray diffractometer (X'Pert MPD PRO, Cu Kα, 40 kV, 40 mA). The resolved diffraction peaks match the crystal data sample perfectly and no characteristic peaks of impurities were observed (Fig. 3).

Heat capacity measurement

Heat capacity measurements of the MgNDC were performed on DSC Q1000 (T-zero DSC-technology, TA Instruments Inc., USA). A mechanical cooling system was

used for the experimental measurement. Dry nitrogen gas with high purity (99.999%) was used as purge gas (50 mL min^{-1}) through the DSC cell. The temperature scale of the instrument was initially calibrated in the standard DSC mode, using the extrapolated onset temperatures of the melting of indium (429.75 K) at a heating rate of 10 K min^{-1}. The energy scale was calibrated with the heat of fusion of indium (28.45 J g^{-1}). The heat capacity calibration was made by running a standard sapphire (α-Al_2O_3) at the experimental temperature. The calibration method was performed at the conditions as follows: (1) sampling interval: 1.00 s/pt; (2) zero heat flow at 328.15 K; (3) equilibrate at 183.15 K; (4) isothermal for 5.00 min; (5) temperature ramp at 10 K min^{-1} to 473.15 K.

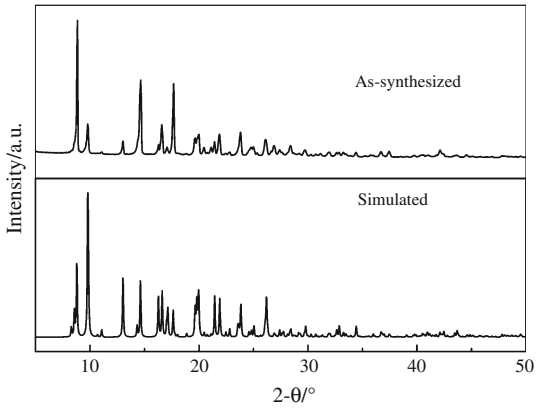

Fig. 3 Experimental and simulated powder XRD pattern of MgNDC

The masses of the reference and sample pans with lids were within 54.25 ± 0.05 mg. Samples were crimped in hermetically sealed aluminum pans with lids using TA's Blue DSC Sample Press. Sample mass was weighed on a METTLER TOLEDO analytical balance (AB135-S, Classic Plus). The mass of the sample was 5.42 mg.

Table 1 The experimental and standard molar heat capacities of sapphire (α-Al_2O_3)

T/K	$C_{p,m}$/J K^{-1} mol^{-1}					Standard value/ J K^{-1} mol^{-1}	RD (%)
	a	*b*	*c*	Standard deviation	Average		
203	50.8	50.7	50.5	0.0011	50.7	51.1	−0.9
213	54.1	53.9	53.8	0.0008	53.9	54.6	−1.3
223	57.3	57.2	57.0	0.0010	57.2	58.0	−1.3
233	60.4	60.1	60.1	0.0005	60.2	61.1	−1.6
243	63.2	62.9	62.8	0.0006	63.0	64.2	−1.9
253	65.9	65.6	65.6	0.0003	65.7	67.1	−2.0
263	68.5	68.2	68.1	0.0007	68.3	69.8	−2.2
273	71.1	70.7	70.6	0.0007	70.8	72.4	−2.2
283	73.7	73.4	73.3	0.0007	73.5	74.9	−1.9
293	76.2	75.8	75.7	0.0004	75.9	77.2	−1.7
303	78.4	78.1	78.0	0.0008	78.1	79.5	−1.7
313	80.1	80.2	80.1	0.0008	80.2	81.6	−1.7
323	82.3	82.2	82.1	0.0009	82.2	83.6	−1.6
333	84.1	84.0	83.8	0.0016	84.0	85.4	−1.7
343	85.8	85.6	85.5	0.0011	85.6	87.2	−1.8
353	87.4	87.2	87.1	0.0006	87.2	88.9	−1.9
363	88.9	88.7	88.7	0.0004	88.8	90.5	−1.9
373	90.4	90.2	90.1	0.0011	90.2	92.0	−2.0
383	92.0	91.6	91.6	0.0004	91.7	93.5	−1.9
393	93.3	93.0	92.9	0.0008	93.1	94.8	−1.9
403	94.4	94.2	94.1	0.0005	94.2	96.1	−2.0
413	95.6	95.4	95.3	0.0008	95.4	97.4	−2.0
423	97.0	96.6	96.6	0.0001	96.7	98.6	−1.9
433	98.0	97.7	97.6	0.0006	97.7	99.7	−1.9
443	99.2	98.8	98.7	0.0008	98.9	100.7	−1.8
453	100.2	99.8	99.8	0.0006	99.9	101.7	−1.8
463	101.1	100.7	100.7	0.0004	100.8	102.7	−1.8
473	102.1	101.7	101.5	0.0014	101.8	103.6	−1.8

Table 2 The experimental and fitted molar heat capacities of MgNDC

T/K	$C_{p,m}$ (exp)/J K^{-1} mol^{-1}					$C_{p,m}$ (fit)/ J K^{-1} mol^{-1}	RD (%)
	a	*b*	*c*	Standard deviation	Average		
205	322.6	321.2	319.1	0.0035	321.0	318.7	−0.7
210	327.7	326.3	324.2	0.0035	326.1	326.9	0.3
215	335.3	333.2	330.9	0.0044	333.1	334.9	0.5
220	343.8	341.5	339.3	0.0045	341.5	342.7	0.4
225	353.0	350.9	348.8	0.0042	350.9	350.4	−0.1
230	361.7	359.4	357.6	0.0041	359.6	357.9	−0.5
235	369.3	366.7	364.5	0.0048	366.8	365.4	−0.4
240	375.4	372.9	370.9	0.0045	373.0	372.9	0.0
245	381.7	379.6	377.8	0.0038	379.7	380.5	0.2
250	389.2	387.1	385.1	0.0041	387.1	388.1	0.2
255	397.5	394.9	392.7	0.0048	395.0	395.8	0.2
260	405.3	402.5	400.5	0.0047	402.7	403.6	0.2
265	413.2	410.7	408.6	0.0045	410.8	411.5	0.2
270	421.2	418.7	416.5	0.0047	418.8	419.5	0.2
275	430.2	427.1	424.6	0.0056	427.3	427.7	0.1
280	439.6	436.6	433.6	0.0059	436.6	435.9	−0.2
285	448.0	445.1	442.0	0.0060	445.0	444.3	−0.2
290	456.8	452.9	450.2	0.0066	453.3	452.7	−0.1
295	465.9	462.1	458.9	0.0069	462.3	461.3	−0.2
300	475.5	472.0	467.9	0.0075	471.8	469.9	−0.4
305	484.7	480.7	476.3	0.0084	480.6	478.5	−0.4
310	493.4	489.3	485.7	0.0077	489.5	487.2	−0.5
315	502.0	497.4	493.2	0.0088	497.5	495.9	−0.3
320	509.5	504.4	500.2	0.0092	504.7	504.7	0.0
325	517.5	513.5	508.5	0.0090	513.2	513.4	0.0
330	525.1	520.5	516.0	0.0090	520.5	522.1	0.3
335	533.7	528.6	524.1	0.0095	528.8	530.7	0.4
340	542.7	538.7	533.7	0.0090	538.4	539.3	0.2
345	551.3	547.3	542.2	0.0090	546.9	547.8	0.2
350	560.4	555.8	550.8	0.0095	555.7	556.3	0.1
355	568.9	563.4	558.3	0.0105	563.6	564.7	0.2
360	577.0	571.4	566.4	0.0105	571.6	573.1	0.3
365	585.6	580.5	574.5	0.0110	580.2	581.4	0.2
370	594.1	588.6	582.5	0.0115	588.4	589.7	0.2
375	602.7	597.1	592.1	0.0105	597.3	598.0	0.1
380	611.8	604.7	599.7	0.0121	605.4	606.2	0.1
385	620.3	614.3	608.7	0.0115	614.4	614.6	0.0
390	630.4	623.9	617.8	0.0125	624.0	623.0	−0.2
395	639.0	631.9	627.4	0.0116	632.8	631.5	−0.2
400	647.5	641.5	636.5	0.0110	641.8	640.2	−0.3
405	656.6	650.6	645.0	0.0115	650.7	649.2	−0.2
410	665.2	659.6	654.1	0.0110	659.6	658.5	−0.2
415	675.8	670.2	665.2	0.0105	670.4	668.2	−0.3
420	686.3	680.8	674.2	0.0120	680.5	678.4	−0.3
425	697.4	691.9	684.8	0.0125	691.4	689.3	−0.3
430	707.5	703.0	694.4	0.0132	701.6	700.8	−0.1
435	718.6	713.0	706.0	0.0125	712.5	713.2	0.1

Table 2 continued

T/K	$C_{p,m}$ (exp)/J K^{-1} mol^{-1}					$C_{p,m}$ (fit)/ J K^{-1} mol^{-1}	RD (%)
	a	*b*	*c*	Standard deviation	Average		
440	731.2	725.6	718.6	0.0125	725.1	726.7	0.2
445	744.3	740.3	731.7	0.0128	738.7	741.2	0.3
450	760.4	755.9	746.8	0.0137	754.4	757.1	0.4
455	778.1	773.0	764.4	0.0137	771.8	774.5	0.3
460	798.7	793.7	784.1	0.0147	792.2	793.6	0.2
465	821.9	815.8	806.8	0.0151	814.8	814.6	0.0
470	848.6	843.6	833.5	0.0153	841.9	837.7	−0.5

Thermal analysis

Thermogravimetric analysis (TG) was carried out on Cahn Thermax 500 from room temperature to 1073 K. The heating rate was 10 K min^{-1} and the flow rate of air was 100 mL min^{-1}. The TG equipment was calibrated by the $CaC_2O_4{\cdot}H_2O$ (99.9%). The mass of MgNDC was 49.44 mg. Mass spectra (MS) were performed on a Multicomponent Online Gas Analyzer GAM 200.

Results and discussion

Heat capacity of standard sapphire (α-Al_2O_3)

Heat capacity measurement is repeated three times under the same condition. The emphasis of this work is to assess the reproducibility and ensure accuracy of the measured data using TMDSC (Q1000). For standard sapphire measurement, the data of three reduplicate experiments and the experimental standard deviation were given in Table 1. The experimental standard deviation is during ±0.0016, which shows that the testing system of TMDSC is steady. Relative deviations have been calculated by the following equation:

$$\mathrm{RD}\,(\%) = 100\% * \left[C_{p,\mathrm{m}}(\mathrm{exp}) - C_{p,\mathrm{m}}(\mathrm{ref})\right]/C_{p,\mathrm{m}}(\mathrm{ref}) \quad (1)$$

where $C_{p,m}$ (exp) is the experimental heat capacities and $C_{p,m}$ (ref) is the referenced heat capacities [18]. The results show that the relative deviation of our calibration data from the recommended value over the whole temperature range was within ±2.2%.

Heat capacities of MgNDC

The data of three reduplicate experiments and the fitted data for MgNDC are given in Table 2. The experimental standard deviations below 0.0153 are obtained and show reasonably good reproducibility in the temperature range from 205 to 470 K. The experimental molar heat capacities curve of MgNDC versus temperature is shown in Fig. 4, it can be seen that the heat capacity of the sample increases with increasing temperature in a smooth and continuous manner in the experimental temperature range. In the whole temperature range, no obvious phase transition can be observed, which indicates that this sample is stable in the experimental temperature range.

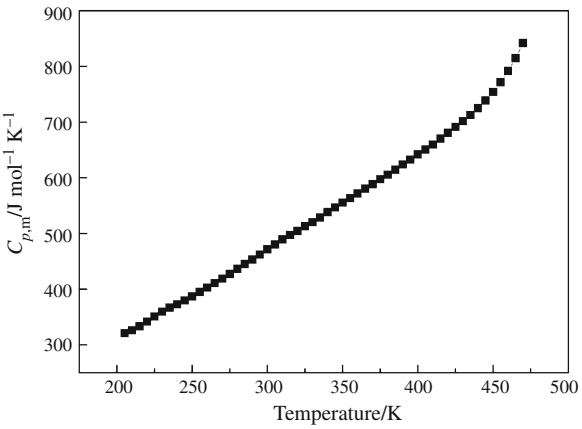

Fig. 4 Molar heat capacities ($C_{p,m}$) of MgNDC as a function of temperature

The molar heat capacities of the sample are fitted to the following polynomial equation of heat capacities ($C_{p,m}$) with reduced temperature (X) using the OriginPro 7.5 software:

From 205 to 470 K,

$$C_{p,\mathrm{m}}\left(\mathrm{J\,K^{-1}\,mol^{-1}}\right) = 535.0 + 227.8\,X - 18.43\,X^2 - 23.58\,X^3 + 61.62\,X^4 + 55.30\,X^5 \quad (2)$$

where $X = (T - 337.5)/132.5$ and T is the experimental temperature, 337.5 is obtained from polynomial $(T_{max} + T_{min})/2$, 132.5 is obtained from polynomial

$(T_{max} - T_{min})/2$, T_{max} is the upper limit (470 K) of the above temperature region, T_{min} is the lower limit (205 K) of the above temperature region. The correlation coefficient is $R^2 = 0.99989$. The relative deviations of all the experimental points from the fitting heat capacities values are within ± 0.7%. Based on Eq. 2, the heat capacity of the sample at 298.15 K was calculated to be 466.7 J mol^{-1} K^{-1}.

Thermodynamic functions of MgNDC

Enthalpy and entropy of substances are basic thermodynamic functions. In terms of the polynomials of molar heat capacity and the thermodynamic relationship, the $(H_T - H_{298.15})$ and $(S_T - S_{298.15})$ of MgNDC was calculated in the temperature ranges from 205 to 470 K with an interval of 5 K relative to the temperature of 298.15 K. The thermodynamic relationships are as follows:

$$H_T - H_{298.15} = \int_{298.15}^{T} C_{p,m} dT \quad (3)$$

$$S_T - S_{298.15} = \int_{298.15}^{T} (C_{p,m}/T) dT \quad (4)$$

The calculated thermodynamic functions $(H_T - H_{298.15})$ and $(S_T - S_{298.15})$ are shown in Table 3.

Thermal stability and decomposition of MgNDC

Thermogravimetric analysis (Fig. 5) shows that three major stages of mass loss occur in the temperature range of 290–1073 K. The curve indicates the mass loss starts at 486 K. The first weight loss step is about 14.9% (calculated 14.5%) in the range of 290–527 K, corresponds to the loss

Table 3 Calculated thermodynamic function data of MgNDC

T/K	$H_T - H_{298.15}$/ kJ mol^{-1}	$S_T - S_{298.15}$/ J K^{-1} mol^{-1}	T/K	$H_T - H_{298.15}$/ kJ mol^{-1}	$S_T - S_{298.15}$/ J K^{-1} mol^{-1}
205	−36.5	−145.0	340	21.1	66.0
210	−34.9	−137.2	345	23.8	73.9
215	−33.2	−129.4	350	26.5	81.8
220	−31.5	−121.6	355	29.3	89.8
225	−29.8	−113.8	360	32.2	97.7
230	−28.0	−106.0	365	35.1	105.7
235	−26.2	−98.3	370	38.0	113.7
240	−24.3	−90.5	375	41.0	121.6
245	−22.5	−82.7	380	44.0	129.6
250	−20.5	−75.0	385	47.0	137.6
255	−18.6	−67.2	390	50.1	145.6
260	−16.6	−59.5	395	53.3	153.6
265	−14.5	−51.7	400	56.4	161.6
270	−12.5	−43.9	405	59.7	169.6
275	−10.3	−36.1	410	62.9	177.6
280	−8.2	−28.3	415	66.2	185.6
285	−6.0	−20.6	420	69.6	193.7
290	−3.7	−12.7	425	73.0	201.8
295	−1.5	−4.9	430	76.5	209.9
298.15	0	0	435	80.0	218.1
300	0.9	2.9	440	83.6	226.3
305	3.2	10.7	445	87.3	234.6
310	5.7	18.6	450	91.1	243.0
315	8.1	26.5	455	94.9	251.4
320	10.6	34.3	460	98.8	260.0
325	13.2	42.2	465	102.8	268.7
330	15.7	50.1	470	106.9	277.5
335	18.4	58.0			

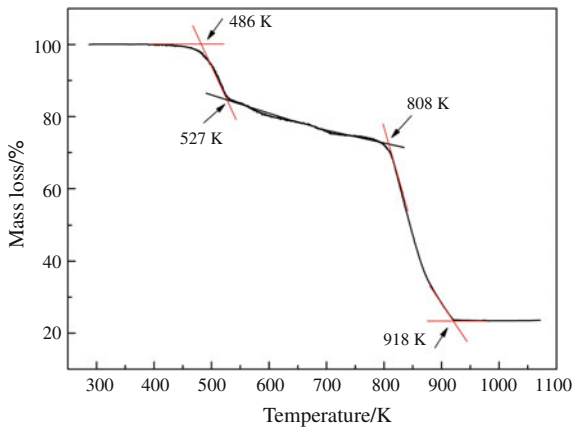

Fig. 5 TG curve of MgNDC in air

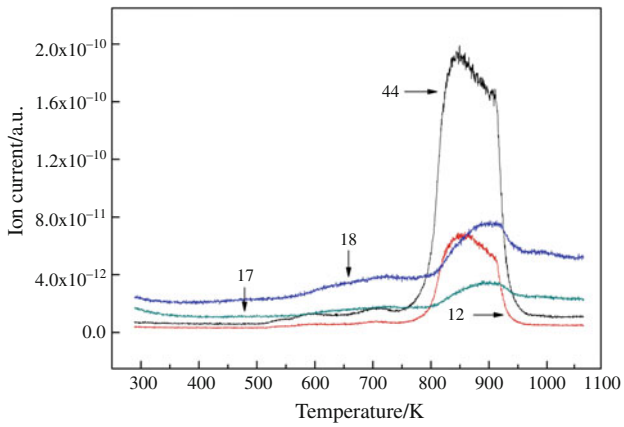

Fig. 6 MS curves (m/z = 12, 17, 18, 44)

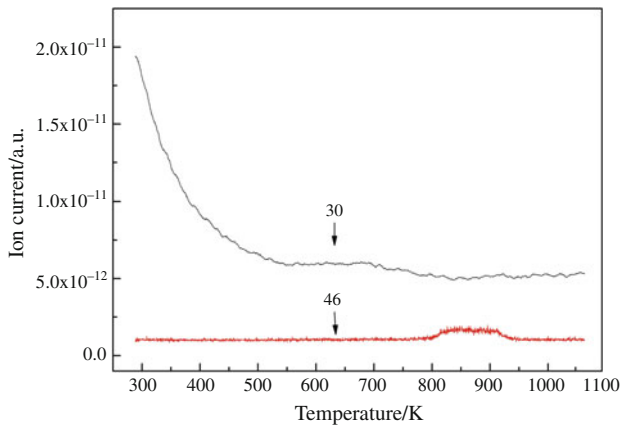

Fig. 7 MS curves (m/z = 30, 46)

of the first DMF molecule per empirical unit. The decomposed products are H_2O (m/z = 17, 18) and NO (m/z = 30), which was validated by TG–MS (Figs. 6, 7). The second step occurs in the region of 527–808 K. The decomposed products of this temperature range are mainly H_2O (m/z = 17, 18) and NO (m/z = 30) and the mass loss is 13.4% (calculated 14.5%) according to the loss of another DMF molecule per empirical unit. The last step occurs in the region of 808–918 K. The decomposed products are mainly H_2O (m/z = 16, 18), CO_2 (m/z = 12, 44), NO (m/z = 30), and NO_2 (m/z = 30, 46), the mass loss is 48.2% (calculated 46.0%) corresponds to the loss of the decomposition of the framework to MgO. The existence of little NO_2 is agree with the incomplete decomposition of DMF molecule in the second step.

Conclusions

In this work, MgNDC has been synthesized solvothermally and characterized by single crystal X-ray diffraction, powder XRD, FT-IR spectra. The molar heat capacities of MgNDC were measured from 205 to 470 K using TMDSC for the first time. The thermodynamic function data relative to the reference temperature (298.15 K) were calculated based on the heat capacities measurements. Moreover, the thermal stability of MgNDC was further investigated by TG–MS.

Acknowledgements The authors gratefully acknowledge the financial support for this work from the National Natural Science Foundation of China (No. 20833009, 20873148, 20903095, 50901070 and U0734005), the National Basic Research Program (973 program) of China (2010CB631303), IUPAC (Project No. 2008-006-3-100), and the State Key Laboratory of Explosion Science and Technology, Beijing Institute of Technology (Grant No. KFJJ10-1Z).

References

1. Murray LJ, Dinca M, Long JR. Hydrogen storage in metal-organic frameworks. Chem Soc Rev. 2009;38:1294–314.
2. Lee J, Farha OK, Roberts J, Scheidt KA, Nguyen ST, Hupp JT. Metal-organic framework materials as catalysts. Chem Soc Rev. 2009;38:1450–9.
3. Liu YY, Zhang J, Xu F, Sun LX, Zhang T, You WS, et al. Lithium-based 3D coordination polymer with hydrophilic structure for sensing of solvent molecules. Cryst Growth Des. 2008;8:3127–9.
4. Bae YS, Mulfort KL, Frost H, Ryan P, Punnathanam S, Broadbelt LJ, et al. Separation of CO2 from CH4 using mixed-ligand metal-organic frameworks. Langmuir. 2008;24:8592–8.
5. Rieter WJ, Taylor KML, An HY, Lin WL, Lin WB. Nanoscale metal-organic frameworks as potential multimodal contrast enhancing agents. J Am Chem Soc. 2006;128:9024–5.
6. Contreras R, Flores-Parra A, Mijangos E, Tellez F, Lopez-Sandoval H, Barba-Behrens N. From mono to polydentate azole and benzazole derivatives, versatile ligands for main group and transition metal atoms. Coord Chem Rev. 2009;253:1979–99.
7. Banerjee D, Kim SJ, Parise JB. Lithium based metal-organic framework with exceptional stability. Cryst Growth Des. 2009;9:2500–3.

8. Liu YY, Zhang H, Sun LX, Xu F, You WS, Zhao Y. Solvothermal synthesis and characterization of a lithium coordination polymer possessing a highly stable 3D network structure. Inorg Chem Commun. 2008;11:396–9.
9. Chen SP, Yang Q, Gao S. Syntheses, characterization and thermal properties of lanthanide complexes with 2-mercaptonicotinic acid. J Therm Anal Calorim. 2009;95:685–9.
10. Leitner J, Ruzicka K, Sedmidubsky D, Svoboda P. Heat capacity, enthalpy and entropy of calcium niobates. J Therm Anal Calorim. 2009;95:397–402.
11. Markin AV, Ruchenin VA, Smirnova NN, Gorina EA, Titova SN, Domrachev GA. Heat capacity and standard thermodynamic functions of a fullerene complex, ((CH3)(3)Si)(12)C-60, over the range from T → 0 K to T = 350 K. J Chem Eng Data. 2010;55:871–5.
12. Dinca M, Long JR. Strong H-2 binding and selective gas adsorption within the microporous coordination solid Mg-3(O2C–C10H6–CO2)(3). J Am Chem Soc. 2005;127:9376–7.
13. Wunderlich B, Jin YM, Boller A. Mathematical-description of differential scanning calorimetry based on periodic temperature modulation. Thermochim Acta. 1994;238:277–93.
14. Wunderlich B. The contributions of MDSC to the understanding of the thermodynamics of polymers. J Therm Anal Calorim. 2006;85:179–87.
15. Danley RL. New modulated DSC measurement technique. Thermochim Acta. 2003;402:91–8.
16. Chau J, Garlicka I, Wolf C, Teh J. Modulated DSC as a tool for polyethylene structure characterization. J Therm Anal Calorim. 2007;90:713–9.
17. Qiu SJ, Chu HL, Zhang J, Qi YN, Sun LX, Xu F. Heat capacities and thermodynamic properties of CoPc and CoTMPP. J Therm Anal Calorim. 2008;91:841–8.
18. Archer DG. Thermodynamic properties of synthetic sapphire (Alpha-Al2O3), standard reference material 720 and the effect of temperature-scale differences on thermodynamic properties. J Phys Chem Ref Data. 1993;22:1441–53.
19. Ginnings DC, Furukawa GT. Heat capacity standards for the range 14-degrees-K to 1200-degrees-K. J Am Chem Soc. 1953;75:522–7.
20. Sheldrick GM. SHELX97, Program for crystal structure refinement. Germany: Göttingen University; 1997.